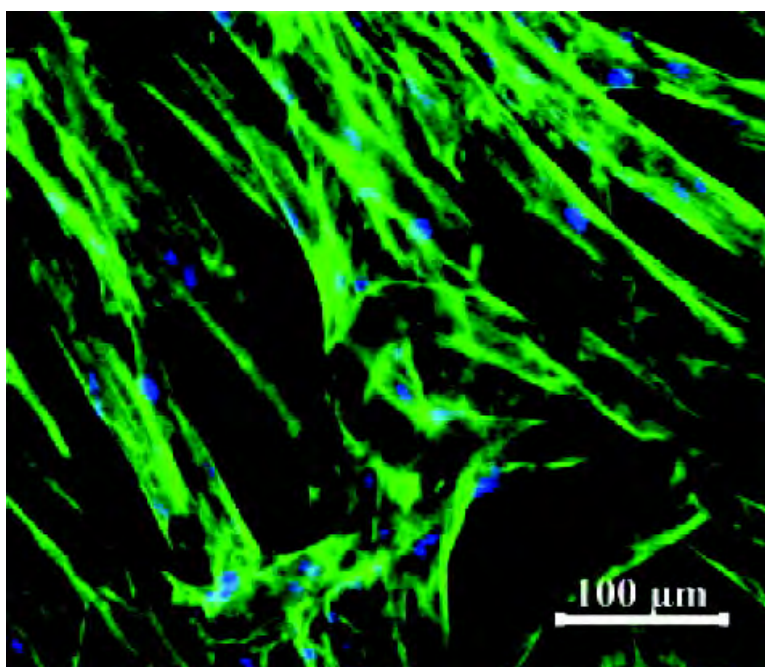Article

Novel Textile Chitosan Scaffolds Promote Spreading, Proliferation, and Differentiation of Osteoblasts

Christiane Heinemann, Sascha Heinemann, Anne Bernhardt, Hartmut Worch, and Thomas Hanke

More About This Article

Additional resources and features associated with this article are available within the HTML version:

- Supporting Information
- Access to high resolution figures
- Links to articles and content related to this article
- Copyright permission to reproduce figures and/or text from this article

View the Full Text HTML

Novel Textile Chitosan Scaffolds Promote Spreading, Proliferation, and Differentiation of Osteoblasts

Christiane Heinemann,* Sascha Heinemann, Anne Bernhardt, Hartmut Worch, and
Thomas Hanke

*Max Bergmann Center of Biomaterials and Institute of Materials Science, Dresden University of
Technology, Budapester Str. 27, D-01069 Dresden, Germany*

Two novel scaffold models made of chitosan fibers were designed, fabricated, and investigated. Raw chitosan fibers were either tightened between plastic rings or were processed into stand-alone scaffolds. Chitosan fiber scaffolds were further modified by coating with a thin layer of fibrillar collagen type I to biologize the surface. Cell culture experiments were carried out using murine osteoblast-like cells (7F2). Confocal laser scanning microscopy (cLSM) as well as scanning electron microscopy (SEM) revealed fast attachment and morphological adaptation of the cells on both the raw chitosan fibers and the collagen-coated scaffolds. Cells were cultivated for up to 4 weeks on the materials and proliferation as well as osteogenic differentiation was quantitatively analyzed in terms of lactate dehydrogenase (LDH) and alkaline phosphatase (ALP) activity. We found a 14−16-fold increase of cell number and the typical pattern of ALP activity, whereas the collagen coating does not remarkably influence these parameters. The maintenance of osteogenic phenotype on the novel materials was furthermore confirmed by immunostaining of osteocalcin and study of matrix mineralization. The feature of the collagen-coated but also the raw chitosan fiber scaffolds to support the attachment, proliferation, and differentiation of osteoblast-like cells suggest a potential application of chitosan fibers and textile chitosan scaffolds for the tissue engineering of bone.

Introduction

During the last few years, technical textile technologies have attracted more and more attention in regenerative medicine. Established processing technologies like weaving, stitching, and knitting allow the fabrication of adapted medical products.[1] Furthermore, these technologies enabled the fabrication of constructs that fulfill most requirements of an ideal scaffold system.[2,3] One of the most important advantages over conventional foam-like scaffolds is the higher ratio of surface area to volume. This feature supports the adhesion of cells and the diffusion of nutrients inside the scaffold.[4]

Until now, synthetic polymers have been successfully applied for the tissue engineering of bone, cartilage, heart valves, bladder, and liver. Mostly, aliphatic polyesters (PGA, PLLA) or copolymers (PLGA) were used.[4−8] Additionally, positive results were attained for the application of polyhydroxybutyrate (PHB), a polyester of bacterial origin with properties similar to that of synthetic polypropylene.[9,10] However, synthetic polymers, generally used for tissue engineering devices, exhibit some properties that may have negative effects on the successful application. For example, the cell adhesion on untreated polymers is insufficient, the hydrophobic surface prevents cell ingrowth, and lack of functional residues complicates chemical modification.[11] Furthermore, acidic degradation products occurring in vivo often cause inflammation.[12]

Due to these complications, the focus switched to the usage of polymers from natural sources, including proteins and polysaccharides. Especially the protein collagen, an essential element of extracellular matrices, is well-established in tissue engineering applications. The material consists of collagen fibrils

composed of a staggered array of tropocollagen molecules, each built up from three helices of amino acid chains.[13] The structure results in a useful combination of positive features like solubility, biodegradability, low immunogenicity, and good mechanical properties, which allows high processibility and a wide range of uses.

Chitosan is a polysaccharide that is produced by deacetylation of naturally occurring chitin. Despite its poor solubility in water, chitosan has become a common substance in biomaterials research with promising pharmaceutical perspectives.[14] The biocompatible and biodegradable material is easy to functionalize and its degradation products are nontoxic.[15] Hydrolases like lysozyme, pektinase, cellulose, hemicellulase, lipase, chitinase, and chitosanase are able to depolymerize chitosan.[14,16] In the human body, the degradation by the body's own lysozymes is recognized as the dominating process.[17] Hydrolysis results in the formation of chitosan oligomers.[18]

Films, gels, as well as porous sponge-like scaffolds made of chitosan are widely investigated and show a therapeutic potential in regenerative medicine.[19] Recently, porous chitosan/hydroxyapatite scaffolds for bone tissue engineering have been developed.[20] Porous scaffolds made of pure chitosan or chitosan-based composites are generally prepared by the freeze-drying method, but also freeze-gelation or freeze−extraction methods can be used.[21] Technologies for chitosan fiber production have been established through the last two decades.[22] The electrospinning process can be used for the production of thin chitosan fibers down to the nanometer scale.[23] In many studies, chitosan fibers are made by the wet-spinning process, which produces fibers by first dissolving the polymer in a solvent (e.g., acetic acid) and then extruding the polymer solution via dies into a nonsolvent (e.g., aqueous sodium hydroxide). The polymer precipitates as a fiber, which can be washed, drawn, and dried

* To whom correspondence should be addressed. E-mail: christiane.heinemann@tu-dresden.de.

to form fibers. Scaffolds prepared from chitosan fibers could combine adequate porous structure with sufficient degradability and mechanical properties.

Owing to the combination of positive properties chitosan is recognized as a valuable base material for various biomedical applications. A special impact for tissue engineering applications is envisaged for the chitosan-based fibers that can be processed in three-dimensional scaffolds with adaptable properties by using established textile techniques. However, until now there have been few reports on the application of textile chitosan scaffolds as a substrate for bone tissue engineering. Tuzlakoglu et al. used a chitosan fiber mesh as a substrate for cultivation of SaOs-2 cells.[24] The results confirmed that the material does not show cytotoxic effects. Adhesion and proliferation of the cells was confirmed qualitatively by SEM investigations. Further studies demonstrated that the cell activity can be increased by a biomimetic apatite-like coating.[25]

In this study we used raw chitosan fibers as a scaffold model for cell culture experiments. Furthermore, we coated the scaffolds with fibrillar collagen type I to achieve biologization whose influence on cell behavior is investigated. We demonstrated the process of initial cell adhesion by using cLSM and SEM. Cell proliferation, maintenance of the osteogenic phenotype and mineralization over a long-term cultivation period were analyzed by quantitative biochemical assays.

Materials and Methods

Chitosan Fiber Scaffolds and Collagen Coating. Chitosan fibers were provided in form of a multifilament yarn by Heppe GmbH, Germany. The raw material is crab chitin which is deacetylated (DD 90%) to chitosan of molecular weight between $100000-200000$. The wet spinning technique was used to produce the fibers that possess line density 1.23 mg/cm, breakdown strength 1.46 g/d, uneven rate of breakdown strength 12.1%, extensibility 12.8%, and uneven rate of breakdown extensibility 23.3%. For microscopic analyses the chitosan fibers were tightened between the plastic rings of Minusheet-Holders (inner diameter 10 mm). Stand-alone scaffolds (diameter 10 mm) for determination of chemical properties and cell culture experiments were processed by using the crown knot technique, which is illustrated in Supporting Information.

Bovine tropocollagen type I (Invitrogen) was assembled into a fibrillar coating directly on the scaffolds. Therefore, equal volumes of tropocollagen solution (0.7 mg/mL in 10 mM acetic acid) and physiological buffer solution (10 mM KH_2PO_4, 50 mM Na_2HPO_4, pH 7.4) were mixed at 4 °C.[26] After completely soaking the chitosan scaffolds in the mixture, fibrillation of the collagen was carried out at 37 °C. After 24 h, the coated scaffolds were rinsed in deionized water and lyophilized in a Christ Alpha 1–4 machine. To stabilize the coating, chemical cross-linking of the collagen was performed using *N*-(3-dimethylaminopropyl)-*N'*-ethylcarbodiimide (EDC) and *N*-hydroxysuccinimide (NHS). The scaffolds were incubated in EDC/NHS solution for 5 h, followed by extensive washing in 0.1 M Na_2HPO_4 (pH 9.0), 4 M NaCl, and deionized water to remove residuals. The procedure was finished by freeze-drying the coated chitosan scaffolds.

Cell Culture. A part of the scaffolds was sterilized by ethylene oxide. Residual gas was allowed to evaporate for two weeks before usage of the sterilized scaffolds. Gamma-irradiation (25 kGy) was used as a standard to sterilize the uncoated and collagen-coated chitosan scaffolds before starting the cell culture experiments.

Murine osteoblast-like cell line 7F2 was obtained from the American type Culture Collection (ATCC). Cells were expanded in minimal essential medium (α-MEM) supplemented with 10% fetal calf serum (FCS), 2 mM L-glutamine, and the antibiotics penicillin (100 U/mL) and streptomycin (100 U/mL) in a humidified atmosphere (37 °C, 7% CO_2). Medium and all supplements were obtained from Biochrom, Germany.
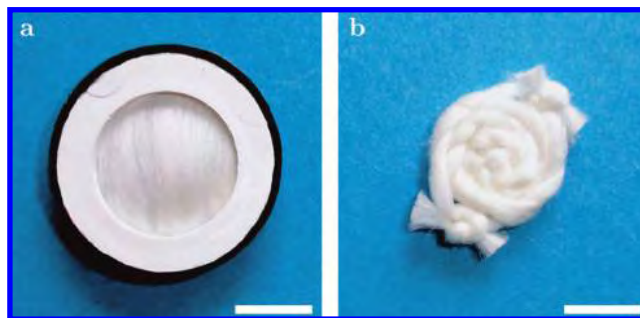

Figure 1. Mesh-like scaffold derived by fixing chitosan fibers in a Minusheet-Holder (a) and stand-alone chitosan scaffold derived by textile processing techniques (b). Space bar represents 5 mm.

The scaffolds were placed in 48-well plates and soaked in cell culture medium for 24 h to prevent floating. After removing the medium, 40 μL of cell suspension (2500 cells per μL) was placed onto each scaffold. Cells were allowed to adhere for 30 min in the incubator before filling up the wells with additional medium. On third day, cells were induced for mineralization by addition of 7.4 mM β-glycerol phosphate (Sigma) to the medium.[27] The medium was changed every third day. The common LIVE/DEAD viability/cytotoxicity kit (Invitrogen) was used to check the suitability of the sterilization procedure.

Microscopy. SEM was used to characterize the uncoated and collagen-coated chitosan scaffolds before and after cell culture experiments, respectively. The cell seeded samples were washed with 37 °C phosphate buffered saline (PBS) twice and then fixed with 3.7% formaldehyde (Sigma) at 4 °C. Dehydration was performed by series of graded ethanol solutions before critical-point drying using a CPD 030 apparatus (BAL-TEC AG, Liechtenstein). The samples were mounted on stubs and sputtered with gold in a Balzers SDC 050 coater. Microscopy was carried out using a Philips ESEM XL 30 in Hi-Vac mode by applying an acceleration voltage of 3 kV and detecting secondary electrons for imaging. Additionally, energy dispersive X-ray (EDX) mapping was performed in order to visualize distribution of calcium and phosphorus as typical elements of cell-formed mineral.

Cell morphology, spreading, orientation, and growth were evaluated using cLSM. After washing and fixing, the cells were permeabilized with 0.2% Triton-X-100 in PBS and blocked with 1% bovine serum albumin (BSA, Sigma) for 30 min. Cytoskeletal actin was stained with AlexaFluor 488-Phalloidin (Invitrogen), and cell nuclei was stained with 4′,6-diamidino-2-phenylindole (DAPI, Sigma). In the case of collagen-coated chitosan fibers, anti-bovine collagen type I (mouse IgG; Sigma) was linked to the collagen coating. AlexaFluor 546 conjugated goat anti-mouse IgG (Invitrogen) was used as the secondary antibody for staining. To visualize differentiation behavior, osteocalcin was labeled with anti-mouse osteocalcin (goat IgG; Santa Cruz Biotechnology), followed by staining with AlexaFluor 488 conjugated donkey anti-goat IgG (Invitrogen). The cytoskeletal actin was stained with AlexaFluor 546-Phalloidin. Collagen was not stained in that case. Tetracycline staining was used in order to visualize matrix mineralization by fluorescent labeling.[28,29] Cells were cultured as described above, except that two days before measurement penicillin/streptomycin in the medium was replaced with 9 μg/mL tetracycline (Sigma). Microscopy was carried out on an upright Axioscop 2 FS mot equipped with a LSM 510 META module (Zeiss, Germany) controlling an argon-ion (Ar$^+$) laser, helium–neon (HeNe) laser, and NIR-femtosecond titanium-sapphire laser for two-photon excitation (Coherent Mira 900F). Excitation of AlexaFluor 488 was carried out at 488 nm (Ar$^+$ laser), the excitation of AlexaFluor 546 at 546 nm (HeNe laser). The NIR-fs-laser laser was used for excitation of both DAPI and tetracycline at 750 nm (2 photon excitation). Fluorescence was recorded at 461 (DAPI) and 550 nm (tetracycline), respectively.

Colorimetric Measurements. Examination of proliferation, differentiation, and mineralization were carried out by a lactate dehydrogenase assay, an alkaline phosphatase assay and a calcium cresolphtha-
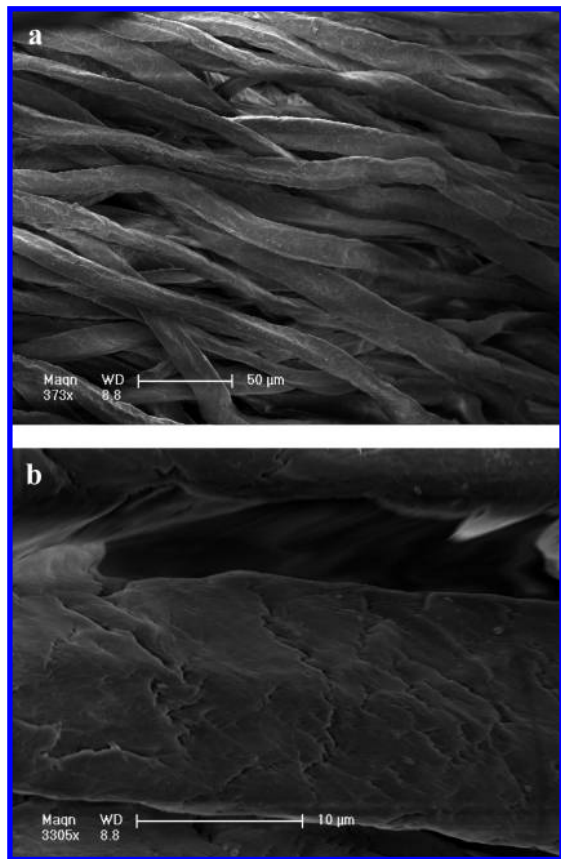
Figure 2. Scanning electron micrographs of native chitosan fibers used for the scaffolds.

Figure 3. Scanning electron micrographs of collagen-coated chitosan fibers.

lein assay, respectively. All measurements were performed with cell lysates after 1, 3, 7, 10, 14, 21, and 28 days of cultivation. Cell lysis was achieved with 1% Triton X-100 (Sigma) in PBS. Ultrasonication (20 s, 80 W) of the scaffolds was applied to support cell lysis. For all colorimetric measurements, a SpectraFluor Plus microplate reader (Tecan, Germany) was used.

Lactate Dehydrogenase (LDH) Activity Assay: Cell proliferation was determined through the total activity of lactate dehydrogenase in the cell lysates using the LDH Cytotoxicity Detection Kit (Takara). An aliquot of cell lysate was mixed with LDH substrate buffer and the enzymatic reaction was stopped after 30 min with 0.5 M HCl. The absorbance was read at 492 nm. The LDH activity was correlated with the cell number using a calibration line of cell lysates with defined cell number.[30,31]

Alkaline Phospatase (ALP) Activity Assay: Cell differentiation was evaluated by the activity of alkaline phosphatase. An aliquot of cell lysate was added to ALP substrate buffer, containing 2 mg/mL *p*-nitrophenyl phosphate (Sigma), 0.1 M diethanolamine, 1 mM $MgCl_2$, 0.1% Triton X-100 (pH 9.8) and the mixture was incubated at 37 °C for 30 min. The enzymatic reaction was stopped by the addition of 0.5 M NaOH, and the absorbance was read at 405 nm. A calibration line was constructed from different concentrations of *p*-nitrophenol.

Calcium Assay: The determination of Ca^{2+} concentration in the lysates was used to evaluate cell mineralization. The method is based on the reaction of Ca^{2+} with *o*-cresolphthalein in an alkaline medium, which results in the formation of a purple-colored complex. Ultrasonication (20 s, 80 W) was used again to support release of the Ca^{2+} from the scaffolds. Lysates were incubated in 0.2 N HCl overnight to release calcium ions which were bound to proteins. The absorbance was measured at 570 nm. A calibration line was constructed from different concentrations of a calcium standard solution.

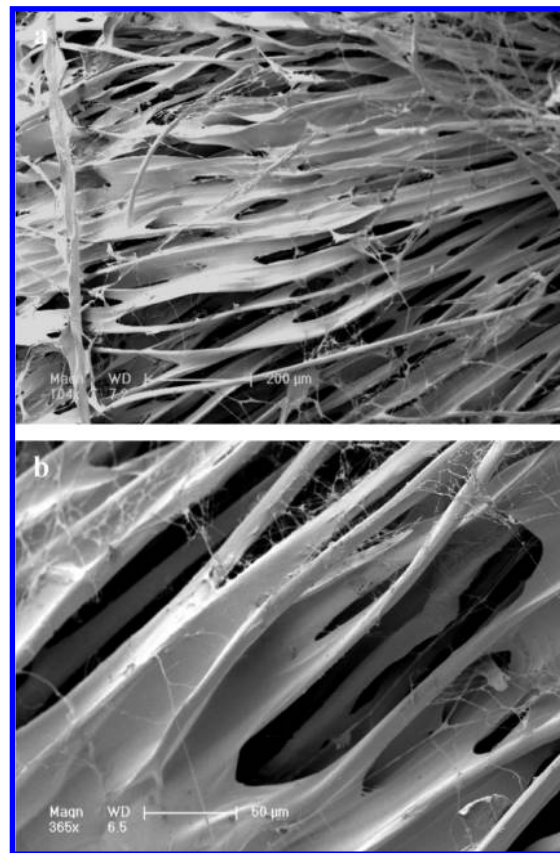*Statistics:* All measurements were collected in triplicate and expressed as means ± standard deviations. Student's *t*-test was employed to assess the statistical significance of results. P-values less than 0.05 were considered significant for all analyses.

Results

Scaffold Characterization. Two different scaffold models were developed to investigate adhesion, proliferation and differentiation of cells of the bone remodelling process cultivated on chitosan fibers. For the mesh-like model (Figure 1a) the parallel aligned chitosan fibers form a smooth surface preferentially suitable for microscopy investigations. Biochemical assays were carried out by cultivating the cells on stand-alone scaffolds of the same chitosan material (Figure 1b). All scaffolds were equal in size and morphology and were easy to handle in cell culture.

The chitosan fibers were characterized using SEM (Figure 2). The fibers are uniform in showing a slightly edged cross-section and a diameter of about 20 μm. Higher magnification of single fibers revealed a rough flaky surface.

A part of the chitosan scaffolds was modified by a coating with fibrillar bovine collagen type I. The morphological characteristics of these samples were also investigated using SEM (Figure 3). The images show that the collagen coating forms smooth layers by spanning two or more single chitosan fibers. A minor amount of the collagen forms fiber networks (Figure 3b). The images also show that collagen layers are formed inside the scaffolds.

Comparison of the Sterilization Methods. Ethylene oxide and gamma irradiation were tested for sterilization of the chitosan scaffolds prior to cell culture experiments. The ethylene oxide method has been recognized to be unsuitable for the chitosan fiber scaffolds, because even after long-term
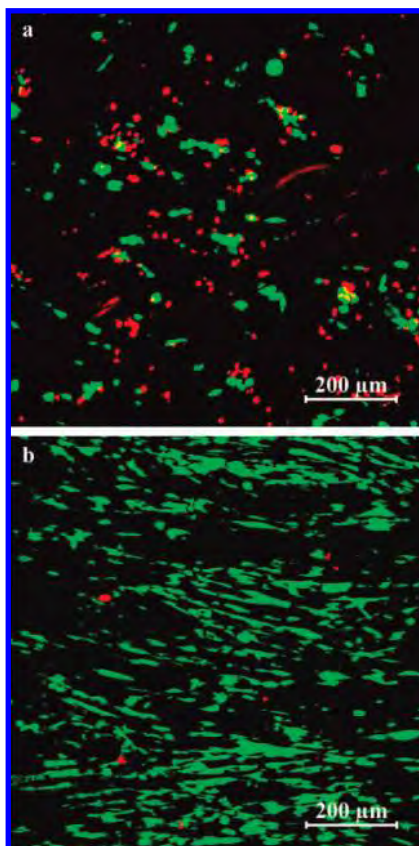
Figure 4. Live/dead staining after 48 h of cultivation 7F2 osteoblasts on ethylene oxide sterilized chitosan scaffolds (a) or gamma-irradiation sterilized chitosan scaffolds (b). Red color indicates dead cells, green indicates living cells.

Figure 5. Three-dimensional reconstructions from cLSM image stacks of 7F2 osteoblasts after 0.5, 1, 4, and 24 h of cultivation on uncoated (left column) as well as collagen-coated (right column) chitosan scaffolds. The actin skeletons (green), the nuclei (blue), and the collagen (red) are visible.

evaporation, toxic residues remain in the porous structure of the scaffolds later causing significant cell death (Figure 4a). However, gamma irradiated scaffolds showed excellent biocompatibility (Figure 4b) and were used for all cell culture experiments within this study. Infrared spectroscopy showed no change in chitosan chemical properties due to irradiation (data not shown).

Cell Adhesion. Cell adhesion on the uncoated and on the collagen-coated chitosan scaffolds was monitored qualitatively by cLSM and SEM. Starting with cLSM, time-dependent spreading of the green fluorescent actin skeleton was observed. Cell nuclei are visible as blue dots. For the coated samples, the collagen was visualized by a red staining (Figure 5).

After 30 min of cultivation, the cells exhibit a spherical morphology on both the uncoated and the collagen-coated scaffolds. However, on the uncoated samples, the cells show initial formation of filopodia demonstrating the start of spreading. A total of 1 h after seeding, the cells on the uncoated chitosan scaffolds are slightly spread toward the alignment of the fibers. In contrast, cell spreading of the actin skeleton on the coated scaffolds is more even, which is due to the widespread surfaces formed by the collagen layer (red). The same issue becomes clearer after 4 h of cultivation. The osteoblasts nearly envelop the single fibers of the uncoated scaffold due to proceeding cell spreading. The specified texture is retained explicitly. By contrast, the collagen coating causes the formation of broad closed cell layers. After 24 h, the cells are completely spread on both types of scaffolds. This means that also for the uncoated scaffolds cells evenly span over several single fibers. This fact emphasizes the remarkable adaptability
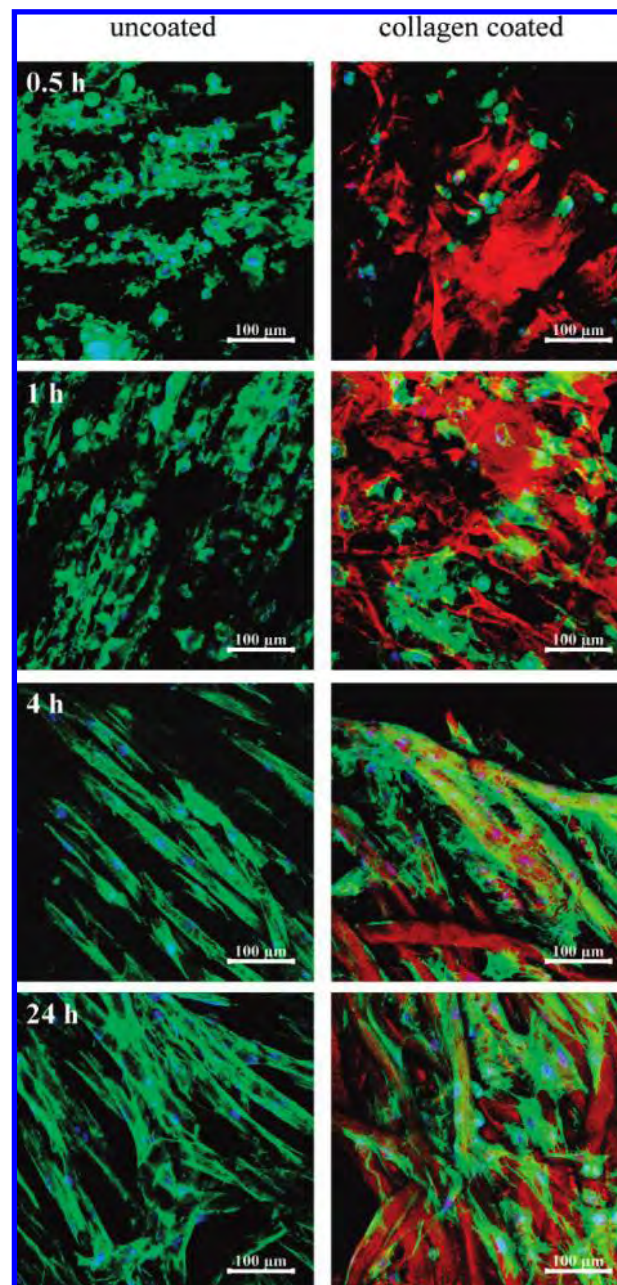
of the cells to the given substrate. Despite that, the spreading toward the fiber's alignment to achieve the maximal contact area is preferred. For the collagen-coated scaffolds, the state is not changed significantly. Closed cell layers, also enveloping one or more coated chitosan fibers, are visible.

Exactly the same samples were critical-point dried and gold sputtered for further analysis using SEM. Images of the uncoated and collagen-coated scaffolds 30 min and 24 h after cell seeding are displayed in Figure 6 to simultaneously visualize the morphology of both the cells and the fibers. Initially, the spherical cells are easy to identify. However, the proceeding spreading complicates the visual distinction from the substrates.

Cell Proliferation and Differentiation. Proliferation and differentiation of the osteoblasts were quantitatively determined over a cultivation period of 28 days. Figure 7 shows that initial
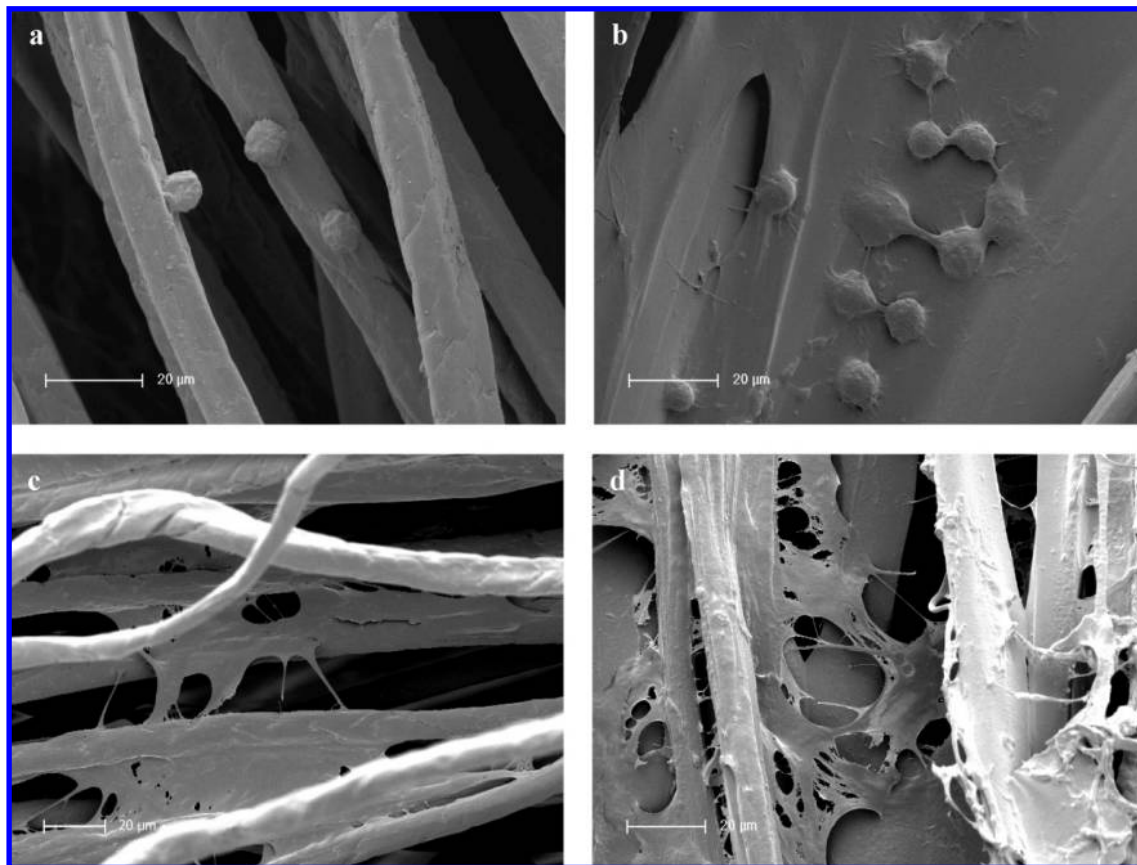
Figure 6. SEM images of 7F2 osteoblasts after 30 min (a, b) and 24 h (c, d) of cultivation on uncoated (left column) as well as collagen-coated (right column) chitosan scaffolds.
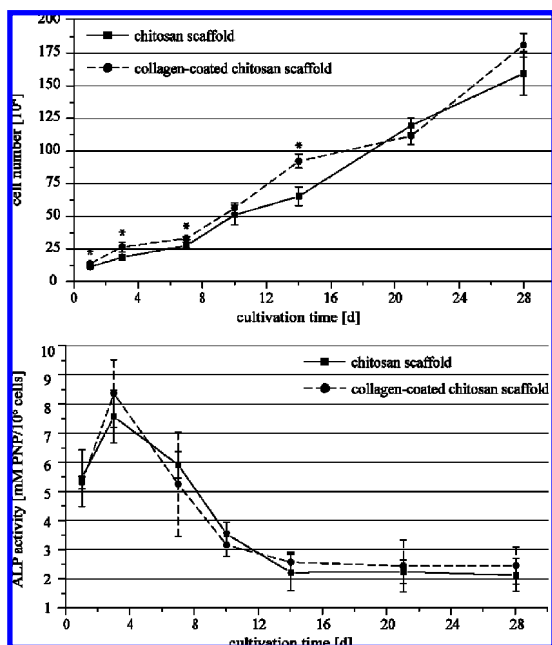

Figure 7. Cell number (calculated from total LDH activity) and specific ALP activity (related to cell number) of 7F2 osteoblasts cultivated on uncoated (solid lines) or collagen-coated (dotted lines) chitosan scaffolds.

proliferation on the collagen-coated scaffolds is slightly higher than on the uncoated scaffolds.

On the supposition of constant enzyme activity, the initial total cell numbers per uncoated or collagen-coated fraction scaffold increased by factors of 14 or 16, respectively. The cell

proliferation was also visualized qualitatively by SEM. Figure 8 shows images of the uncoated chitosan scaffold 24 h after cell seeding (a) and after 14 days of cultivation (b−d). Initially a few, single cells adhere in the loose structure of the scaffold. Owing to proceeding proliferation cell density increases up to the formation of a dense cell layer. After 14 days of cultivation, the chitosan fibers are completely overgrown with cells. Fissures allow the ascertainment that cells also grow inside the scaffold. Qualitatively, the same conditions are present on the collagen-coated scaffolds, but the differentiation between cells and previously deposited collagen becomes more and more difficult during cultivation (images not shown). The results correspond to those of the biochemical assay.

Maintenance of the osteoblastic phenotype during cultivation on the chitosan scaffolds was analyzed by detection of the typical markers ALP (Figure 7) and osteocalcin. Innately, the cells are ripe osteoblasts demonstrated by the specific ALP activity at day 1. The activity reaches the typical maximum around day 3 followed by falling values representing osteocytic differentiation.[32] The collagen coating does not significantly influence the trend. The presence of osteocalcin was verified by immunostaining followed by cLSM. Figure 9 shows the cell nuclei (blue), actin skeleton (red), and osteocalcin (green) of osteoblasts after 28 days of cultivation on the uncoated collagen scaffold. The green fluorescence shows that osteocalcin is present in large amounts concentrated at the surface of the chitosan fibers. The sectional planes confirm the position of osteocalcin as illustrated by the *ortho*-representation of the same image in panel b of Figure 9. Detection of osteocalcin on the collagen-coated scaffolds is slightly disturbed by autofluorescence of the scaffold.
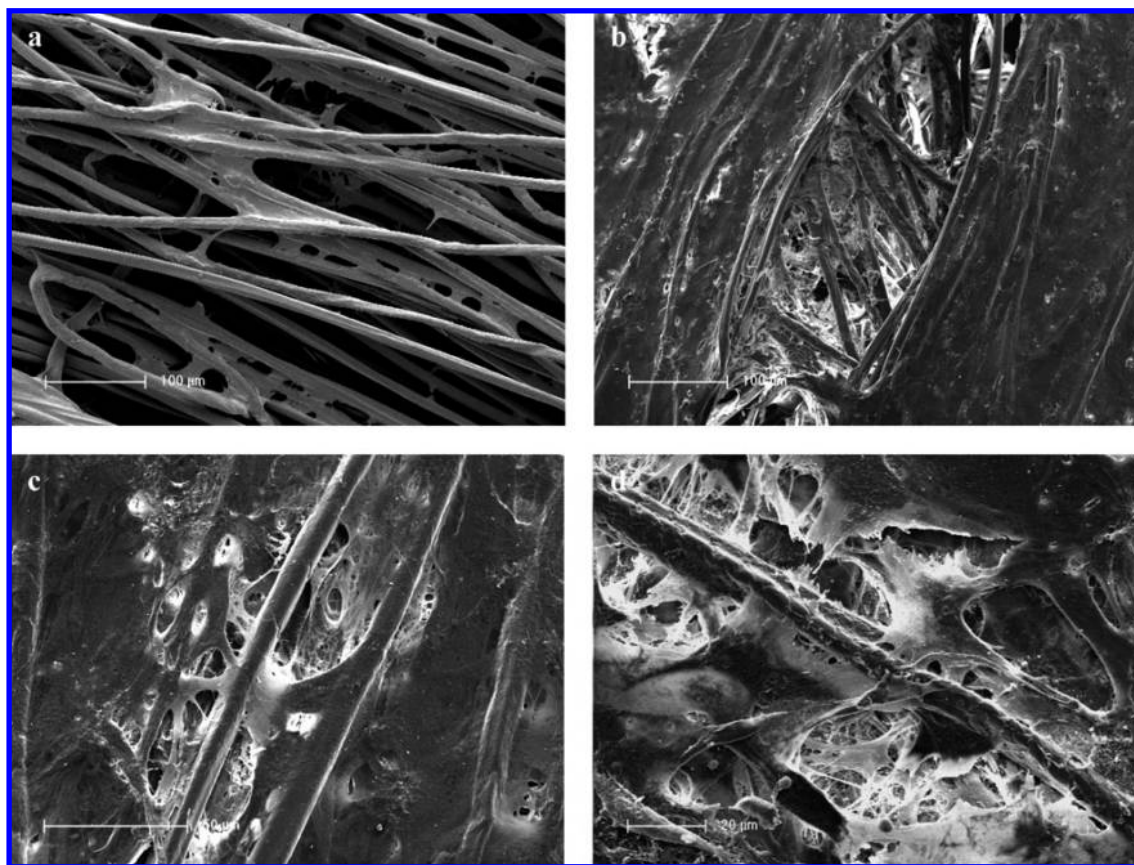
Figure 8. SEM images of 7F2 osteoblasts 24 h (a) or 14 days (b−d) cultivated on the uncoated collagen scaffolds.

Matrix Mineralization. In this study, we tested the mineralization behavior of the cells when cultivated on the uncoated as well as on collagen-coated chitosan scaffolds. Detection of the mineral was performed quantitatively by a colorimetric assay and qualitatively by microscopy as well as EDX spectroscopy.

The calcium concentration in the cell lysates increased continuously from day 10 to day 28 (Figure 10). The levels are significantly higher for the collagen-coated samples. Tetracycline staining (Figure 11), which is based on the incorporation of the fluorescent compound into newly formed calcium phosphate, showed the regular distribution of tetracycline detected in the extracellular matrix formed by the cells during a cultivation period of 28 days on the uncoated chitosan scaffold. Detection of tetracycline on the collagen-coated scaffolds is affected by the autofluorescence of the scaffold again.

The same samples were analyzed using SEM. Figure 12 shows the uncoated and collagen-coated scaffolds overgrown densely by the osteoblasts. In contrast to the SEM images taken after 14 days of cultivation, a large amount of mineral phase was detected, visible as spherical particles or agglomerates embedded in the extracellular matrix. Single particles exhibit a size of about 1−2 μm. EDX mapping of the shown areas revealed an increased presence of calcium and phosphorus located at the particles (Supporting Information). These elements are characteristic for biogenic mineral.

Discussion

Concerning the high demand of bone replacement materials to reconstruct bony defects, numerous biomaterials consisting of different chemical substances were developed for the application in the field of bone tissue engineering. Scaffolds not only function as a delivery vehicle for growth factors and living cells, but also support and regulate bone regeneration by functioning as the fibrillar part of extracellular matrix and maintaining the space and shape of the defect for the regenerated bone.[33] Collagen and chitosan have intrinsic properties that support growth and differentiation of osteoblasts. The effect of the collagen coating on the adhesion, proliferation and differentiation of osteoblasts was investigated and is discussed.

Until now, randomly oriented chitosan fibers forming a nest-like structure have been used as substrate for cell culture experiments.[25] In the present study the chitosan fibers were processed to two scaffold models optimized for quantitative or qualitative analysis methods. Supported chitosan fibers were best suited for microscopy analysis. We used textile techniques for the preparation of uniform stand-alone chitosan scaffolds exhibiting an ordered structure of fiber bundles. The typical structure of the scaffolds will meet the demand of porosity essential for ingrowth of cells and migration of vascular tissue.[33] The rough surface morphology of the individual fibers is determined by the wet spinning process and is similar to that of equivalents known from the literature.[34,35]

Coating tissue engineering scaffolds with collagen is a common procedure to enhance the biocompatibility.[36−38] In this study, a part of the chitosan scaffolds was coated with fibrillar collagen to study its influence on cell adhesion, proliferation, differentiation, and mineralization. The coating procedure modifies both the chemical features and the morphology by forming additional surfaces of different roughness, porosity, and curvature. Both are known to be important for the behavior of cells in contact. In this study, the coating was realized by fibrillation of a tropocollagen solution directly on the chitosan scaffolds. SEM confirmed the formation of collagen layers
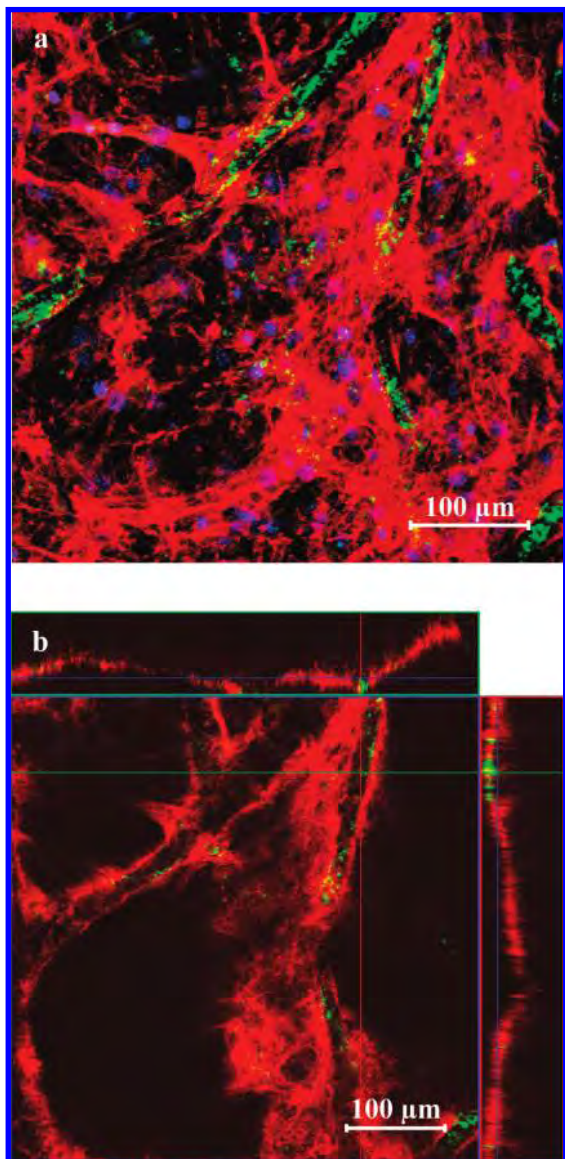
Figure 9. 3D reconstruction from 15 cLSM images of 7F2 osteoblasts after 28 days of cultivation on the uncoated chitosan scaffolds (a). *ortho*-Representation showing a single image of the stack and cross-sections along the colored lines (b). Cell nuclei are visualized blue, actin skeletons red, and osteocalcin green.
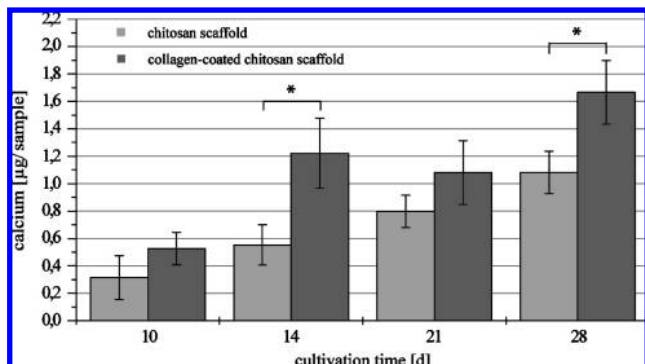

Figure 10. Calcium concentration measured in the lysate of 7F2 osteoblasts cultivated on the uncoated (bright) and collagen-coated (dark) chitosan scaffolds.

Figure 11. Confocal LSM image of the tetracycline (yellow) embedded in mineral formed by 7F2 osteoblasts during 28 days of cultivation on the uncoated scaffold. The chitosan fibers are visualized as violet pseudocolor.

Figure 12. SEM images of cells, extracellular matrix, and the mineral phase formed by 7F2 osteoblasts during 28 days of cultivation on the uncoated (a) or collagen-coated (b) chitosan scaffolds.

spanning between several chitosan fibers. However, the scaffold is not enclosed by the collagen coating, which is important regarding the useful porosit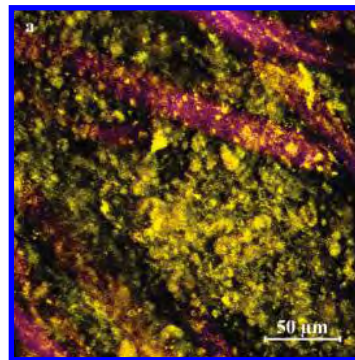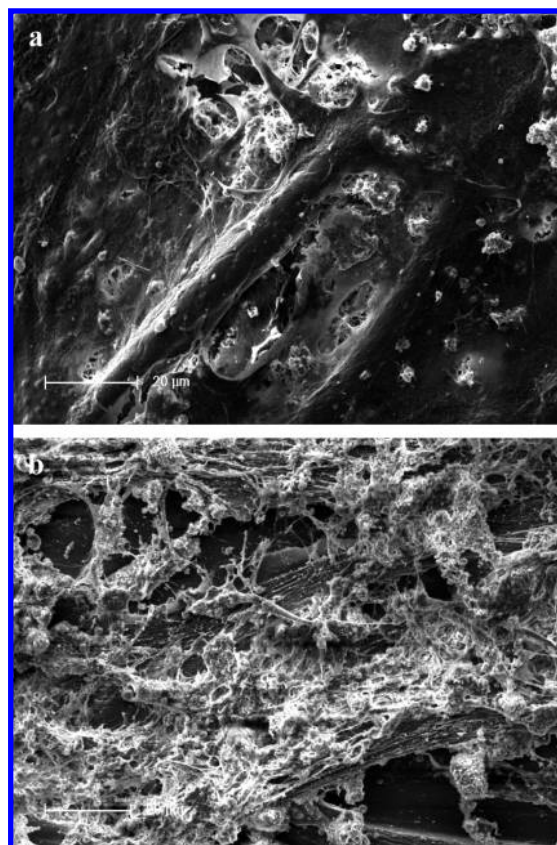y features. Due to the chosen coating technique, the characteristic structure specified by the fiber construct is preserved. Furthermore, the described collagen layers can be found deep inside the scaffolds.

All cell culture experiments, which concentrated on the adhesion, proliferation, and differentiation of the 7F2 osteoblasts, were performed for the uncoated and for the collagen-coated chitosan scaffolds. CLSM showed the cells to be adhered to the uncoated and coated scaffolds within a few minutes. Further imaging confirmed that cell spreading is faster on the collagen-coated scaffolds. Obviously, the additional collagen layers braced in patches facilitate cell spreading. More time is used by the cells to adapt to the cylindrical shape of the uncoated chitosan fibers. After 24 h, on both scaffold types, the cells are well adapted to the morphology of the given substrate by

enveloping the chitosan fibers, which is best demonstrated by the combination of both cLSM and SEM.

Extensive proliferation of the cells is recorded for both scaffold types. During the cultivation time of 28 days, proliferation rate on the uncoated chitosan scaffolds is nearly equal to that on the collagen-coated samples. For chitosan sponges, it is postulated that interactions of the positive chitosan charges and negative charges on the cell surface may enhance the cell's metabolic activity.[39] Further studies confirmed that chitosan enhances angiogenesis and supports growth and differentiation of osteoblasts.[40,41] Microscopy investigations after 28 days of cultivation demonstrated that the osteoblasts form a dense layer around as well as in between the chitosan fibers. Furthermore, the porosity of the scaffold allows ingrowth of the cells. During 28 days of cultivation there are no significant differences between uncoated and collagen-coated chitosan scaffolds.

The phenotype of the cells cultured on chitosan scaffolds was retained as shown by the typical pattern of alkaline phosphatase activity.[42] From the start of cultivation the ALP activity increases significantly. At day 3, β-glycerol phosphate is added to the medium, which is known to promote maturation of the osteoblasts. This means that ALP activity will be down-regulated and the mineralization stage begins.[27] Maintenance of the osteoblastic phenotype was furthermore confirmed by microscopic detection of osteocalcin. The marker is particularly located around the chitosan fibers because the cells directly attached to the fibers are most progressed in growth and expression of extracellular matrix. Cells later developed in the spaces between the fibers also started to express osteocalcin.

Quantitative calcium measurements showed significantly higher levels of calcium on the collagen-coated chitosan scaffolds. This result corresponds to previous reports that described positive effects of collagen coating.[36,43] In particular, Arpornmaeklong et al. reported that the mineral formation of the murine MC3T3 osteoblast cell line is higher when cultivated on collagen-modified chitosan scaffolds than on uncoated chitosan.[44]

Furthermore, the mineralization of the cells was visualized by cLSM using the tetracycline staining and additional SEM. The element composition of the mineralized cell layers on the scaffolds was determined by EDX. The result showed a ratio of the elements calcium and phosphorus that characterizes hydroxyapatite, the major component of the inorganic part of bone.[45]

Conclusion

In the present study, we demonstrated the excellent suitability of chitosan fiber scaffolds for the expansion and differentiation of murine osteoblasts. Collagen I coating of the textile scaffolds did not further improve their biocompatibility. With regard to a potential application in bone tissue engineering, further in vitro investigations should clarify the suitability of the material for the cultivation of human cells. Corresponding experiments with human mesenchymal stem cells are currently performed.

Supporting Information Available. Illustration of the crown knot technique and EDX mapping of cell-formed mineral. This material is available free of charge via the Internet at http://pubs.acs.org.

References and Notes

(1) Czajka, R. *Fibres Text.* **2001**, *13* (1), 49–52.

(2) Sachlos, E.; Czernuszka, J. T *Eur. Cell Mate.* **2003**, *5*, 29–39, discussion 39−40.

(3) Sumanasinghe, M. W. *J. Text. Apparel Technol. Manage.* **2003**, *3* (2), 1–13.

(4) Hutmacher, D. W. *J. Biomater. Sci., Polym. Ed.* **2001**, *12* (1), 107–24.

(5) Laurencin, C. T.; Ambrosio, A. M.; Borden, M. D.; Cooper, J. A., Jr. *Annu. Rev. Biomed. Eng.* **1999**, *1*, 19–46.

(6) Chen, G.; Ushida, T.; Tateishi, T. *J. Biomed. Mater. Res.* **2001**, *57* (1), 8–14.

(7) Chen, G.; Sato, T.; Ushida, T.; Hirochika, R.; Shirasaki, Y.; Ochiai, N.; Tateishi, T. *J. Biomed. Mater. Res. A* **2003**, *67* (4), 1170–80.

(8) Chen, G.; Sato, T.; Ushida, T.; Ochiai, N.; Tateishi, T. *Tissue Eng.* **2004**, *10* (3−4), 323–30.

(9) Hrabak, O. *FEMS Microbiol. Lett.* **1992**, *103*, 251–68.

(10) Wollenweber, M.; Domaschke, H.; Hanke, T.; Boxberger, S.; Schmack, G.; Gliesche, K.; Scharnweber, D.; Worch, H. *Tissue Eng.* **2006**, *12* (2), 345–59.

(11) Gunatillake, P. A.; Adhikari, R. *Eur. Cell Mater.* **2003**, *5*, 1–16, discussion 16.

(12) Taylor, M. S.; Daniels, A. U.; Andriano, K. P.; Heller, J. *J. Appl. Biomater.* **1994**, *5* (2), 151–7.

(13) Heinemann, S.; Ehrlich, H.; Douglas, T.; Heinemann, C.; Worch, H.; Schatton, W.; Hanke, T. *Biomacromolecules* **2007**, *8* (11), 3452–7.

(14) Kumar, M. N.; Muzzarelli, R. A.; Muzzarelli, C.; Sashiwa, H.; Domb, A. J. *Chem. Rev.* **2004**, *104* (12), 6017–84.

(15) Kurita, K. *Mar. Biotechnol.* **2006**, *8* (3), 203–26.

(16) Fukamizo, T. *Curr. Protein Pept. Sci.* **2000**, *1* (1), 105–24.

(17) Varum, K. M.; Myhr, M. M.; Hjerde, R. J.; Smidsrod, O. *Carbohydr. Res.* **1997**, *299* (1−2), 99–101.

(18) Kohn, P.; Winzler, J.; Hoffman, R. C. *J. Biol. Chem.* **1962**, *237*, 304–8.

(19) Shi, C.; Zhu, Y.; Ran, X.; Wang, M.; Su, Y.; Cheng, T. *J. Surg. Res.* **2006**, *133* (2), 185–92.

(20) Manjubala, I.; Ponomarev, I.; Wilke, I.; Jandt, K. D. *J. Biomed. Mater. Res. B* **2008**, *84* (1), 7–16.

(21) Hsu, S. H.; Whu, S. W.; Hsieh, S. C.; Tsai, C. L.; Chen, D. C.; Tan, T. S. *Artif. Organs* **2004**, *28* (8), 693–703.

(22) Qin, Y.; Agboh, O. C. *Med. Device Technol.* **1998**, *9* (10), 24–8.

(23) Ohkawa, K.; Cha, D.; Kim, H.; Nishida, A.; Yamamoto, H. *Macromol. Rapid Commun.* **2004**, *25*, 1600–5.

(24) Tuzlakoglu, K.; Alves, C. M.; Mano, J. F.; Reis, R. L. *Macromol. Biosci.* **2004**, *4* (8), 811–9.

(25) Tuzlakoglu, K.; Reis, R. L. *J. Mater. Sci.: Mater. Med.* **2007**, *18* (7), 1279–86.

(26) Douglas, T.; Heinemann, S.; Bierbaum, S.; Scharnweber, D.; Worch, H. *Biomacromolecules* **2006**, *7* (8), 2388–93.

(27) Thompson, D. L.; Lum, K. D.; Nygaard, S. C.; Kuestner, R. E.; Kelly, K. A.; Gimble, J. M.; Moore, E. E. *J. Bone Miner. Res.* **1998**, *13* (2), 195–204.

(28) zur Nieden, N. I.; Kempka, G.; Ahr, H. J. *Differentiation* **2003**, *71* (1), 18–27.

(29) Holy, C. E.; Shoichet, M. S.; Davies, J. E. *J. Biomed. Mater. Res.* **2000**, *51* (3), 376–82.

(30) Sepp, A.; Binns, R. M.; Lechler, R. I. *J. Immunol. Methods* **1996**, *196* (2), 175–80.

(31) Curran, J. M.; Chen, R.; Hunt, J. A. *Biomaterials* **2006**, *27* (27), 4783–93.

(32) Robins, S. P. *Biochemical markers in bone turnover*; Chapman and Hall: London, 1997; pp 231−50.

(33) Kuboki, Y.; Jin, Q.; Takita, H. *J. Bone Joint Surg. Am.* **2001**, *83A* Suppl 1, (Pt 2), S105–15.

(34) Agboh, O. C.; Qin, Y. *Polym. Appl. Technol.* **1997**, *8*, 355–65.

(35) Knaul, J.; Hooper, M.; Chanyi, C.; Creber, K. A. M. *J. Appl. Polym. Sci.* **1998**, *69*, 1435–44.

(36) Kleinman, H. K.; Klebe, R. J.; Martin, G. R. *J. Cell Biol.* **1981**, *88* (3), 473–85.

(37) Pachence, J. M. *J. Biomed. Mater. Res.* **1996**, *33* (1), 35–40.

(38) Zhang, Y. Z.; Venugopal, J.; Huang, Z.-M.; Lim, C. T.; Ramakrishna, S. *Biomacromolecules* **2005**, *6*, 2583–2589.

(39) Ma, J.; Wang, H.; He, B.; Chen, J. *Biomaterials* **2001**, *22*, 331–6.

(40) Klokkevold, P. R.; Vandemark, L.; Kenney, E. B.; Bernard, G. W. *J. Peridontol.* **1996**, *67*, 1170–1175.

(41) Lahiji, A.; Sohrabi, A.; Hungerford, D. S.; Frondoza, C. G. *J. Biomed. Mater. Res.* **2000**, *51*, 586–95.

(42) Hughes, F. J.; Aubin, J. E. *Culture of cells of the osteoblast linage*; Chapman and Hall: London, 1997; pp 1−49.

(43) Salasznyk, R. M.; Williams, W. A.; Boskey, A.; Batorsky, A.; Plopper, G. E. *J. Biomed. Biotechnol.* **2004**, *2004* (1), 24–34.

(44) Arpornmaeklong, P.; Suwatwirote, N.; Pripatnanont, P.; Oungbho, K. *Int. J. Oral Surg.* **2007**, *36* (4), 328–37.

(45) Sharma, B.; Elisseeff, J. H. *Ann. Biomed. Eng.* **2004**, *32* (1), 148–59.